

## EJC-independent degradation of nonsense immunoglobulin- $\mu$ mRNA depends on 3' UTR length

Marc Bühler<sup>1,2</sup>, Silvia Steiner<sup>1</sup>, Fabio Mohn<sup>1,2</sup>,  
Alexandra Paillusson<sup>1</sup> & Oliver Mühlemann<sup>1</sup>

**Inconsistent with prevailing models for nonsense-mediated mRNA decay (NMD) in mammals, the mRNA levels of immunoglobulin- $\mu$  (Ig- $\mu$ ) genes with premature termination codons (PTCs) in the penultimate exon are still reduced by NMD when the intron furthest downstream is deleted. As in yeast, this exon junction complex-independent NMD of Ig- $\mu$  mRNAs depends on the distance between the termination codon and the poly(A) tail and suggests an evolutionarily conserved mode of PTC recognition.**

NMD is a post-transcriptional quality-control mechanism in eukaryotic gene expression that degrades transcripts containing premature termination codons (PTCs) in a translation-dependent manner, thereby preventing cells from producing potentially deleterious C-terminally truncated proteins<sup>1,2</sup>. A key question in NMD is which features distinguish a termination codon that is 'premature' and therefore elicits NMD from those that are 'correct' and do not trigger

NMD. Although the key NMD factors Upf1, Upf2 and Upf3 (also called SMG2, SMG3 and SMG4, respectively) are conserved from yeast to human, current models for NMD differ widely between different organisms. In mammals, it has been postulated that termination codons only elicit NMD when they are located >50–55 nucleotides (nt) upstream of the most downstream exon-exon junction (reviewed in ref. 2). This suggestion, together with the discovery that splicing deposits a protein complex called the exon-junction complex (EJC) 20–24 nt upstream of an exon-exon junction, have led to the model that termination codons are recognized as premature if they are located upstream of an EJC. The current model for mammalian NMD predicts that these EJCs are removed from a messenger ribonucleoprotein particle (mRNP) during the first round of translation. Upon translation termination at an upstream termination codon, the remaining EJCs have been proposed to interact with the stalled ribosome via the Upf *trans*-acting factors, which ultimately leads to degradation of the mRNA (ref. 2 and references therein). However, PTCs as close as 8–10 nt upstream of the last junction still elicit NMD in T cell receptor- $\beta$  (TCR $\beta$ ) or Ig- $\mu$  transcripts expressed in human tissue-culture cells, although to a lesser extent than PTCs located >55 nt upstream of the most downstream exon-exon junction<sup>3,4</sup>. Additional examples that violate the '50-nt boundary rule' have also been reported<sup>5–9</sup>.

To investigate the mechanisms by which B cells prevent the expression of unproductively rearranged immunoglobulin alleles, we developed an Ig- $\mu$  minigene (mini $\mu$ ) driven by the  $\beta$ -actin promoter,

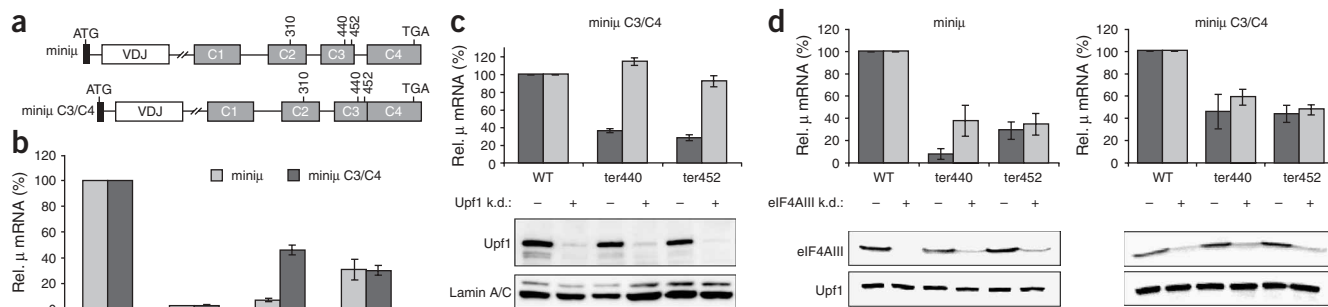


**Figure 1** NMD does not require a downstream intron or the EJC factor eIF4AIII. (a) Schematic representations of Ig- $\mu$  minigenes. Start codon (ATG) and physiological termination codon (TGA) are indicated; numbers mark the amino acid positions where a PTC was generated by a site-directed point mutation. (b) Relative levels of Ig- $\mu$  mRNA expressed from the indicated mini $\mu$  constructs were measured 48 h post transfection by real-time RT-PCR, as described in **Supplementary Methods** online. (c) From HeLa cells depleted of Upf1 (+, light bars) or control cells (-, dark bars), relative Ig- $\mu$  mRNA levels were measured 96 h post transfection as in b. Upf1 knockdown (k.d.) was assessed by western blotting (gel at bottom). (d) From HeLa cells depleted of the EJC factor eIF4AIII (+) or from control cells (-), relative Ig- $\mu$  mRNA levels of the indicated full-length mini $\mu$  (left panel) and mini $\mu$  C3/C4 constructs (right panel) were measured 72 h post transfection as in b. eIF4AIII knockdown was assessed by western blotting (gels at bottom). Average mRNA levels and s.d. were derived from at least three real-time PCR runs.

<sup>1</sup>Institute of Cell Biology, University of Bern, Baltzerstrasse 4, CH-3012 Bern, Switzerland. <sup>2</sup>Present addresses: Harvard Medical School, Dept. of Cell Biology, LHRB Room 517, 240 Longwood Avenue, Boston, Massachusetts 02115, USA (M.B.) and Friedrich Miescher Institute for Biomedical Research, PO Box 2543, CH-4002 Basel, Switzerland (F.M.). Correspondence should be addressed to O.M. (oliver.muehlemann@izb.unibe.ch).

Received 29 September 2005; accepted 6 March 2006; published online 23 April 2006; doi:10.1038/nsmb1081

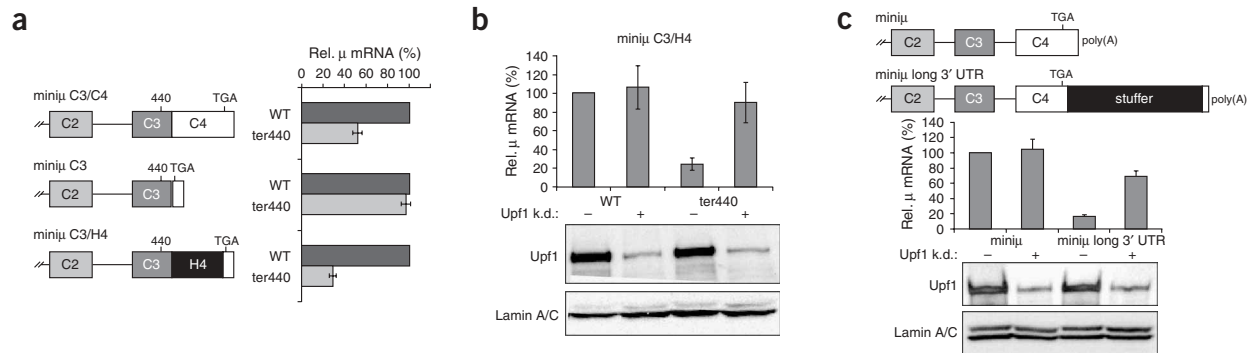


**Figure 2** The distance between the termination codon and the poly(A) tail determines whether NMD is elicited. **(a)** Relative Ig-μ mRNA levels of indicated constructs were measured 48 h post transfection as in **Figure 1**. **(b)** From HeLa cells depleted for human Upf1 (+) or control cells (-), relative Ig-μ mRNA levels of WT or ter440 miniμ C3/H4 were measured 96 h post transfection. Upf1 knockdown (k.d.) was assessed by western blotting (gel at bottom). **(c)** Extension of the 3' UTR triggers NMD. A 1.3-kilobase stuffer fragment was inserted into the 3' UTR of miniμ, giving miniμ long 3' UTR. PTC-free miniμ or miniμ long 3' UTR was transfected together with pSUPERpuro plasmids targeting human Upf1 (+) or pSUPERpuro-scrambled as a control (-), as in **b**. Upf1 knockdown was assessed as in **b**. Average mRNA levels and s.d. were derived from at least three real-time PCR runs.

which allows its expression in nonlymphoid cells (**Fig. 1a**)<sup>3</sup>. We introduced point mutations to generate PTCs at various positions within the open reading frame, transiently expressed these different constructs in HeLa cells and measured their steady-state mRNA levels by real-time reverse-transcription (RT)-PCR. As predicted by the 50-nt boundary rule, a PTC in exon C2 at amino acid 310 (ter310) or in exon C3 (ter440, 67 nt upstream of the most downstream exon-exon junction) results in a greatly reduced mRNA level. However, PTCs only 31 nt (ter452) or 10 nt (ter459) upstream of the most downstream exon-exon junction still led to two- to four-fold reductions in mRNA levels compared to the mRNA levels of the PTC-free wild-type (WT) construct (**Fig. 1b** and ref. 3). Deletion of the intron between exons C3 and C4 (**Fig. 1a**, miniμ C3/C4) did not alter the roughly three-fold reduction of mRNA elicited by ter452, demonstrating that ter452 triggers mRNA downregulation independently of a downstream splicing event and thus does not require a downstream EJC. Notably, ter440, which in miniμ resides just upstream of the 50-nt boundary and leads to a 15-fold reduced mRNA level, still causes a two-fold mRNA reduction when the downstream intron is deleted (miniμ C3/C4). We conclude that PTCs in Ig-μ lead to reduced mRNA levels even in the absence of a downstream intron, but that the mRNA levels are reduced a further seven-fold when the PTC is followed by an intron > 55 nt downstream. Correct splicing of the miniμ C3/C4 constructs was confirmed by RT-PCR (**Supplementary Fig. 1** online) and sequencing of the RT-PCR products (data not shown). Because dependence on mRNA translation and the Upf1 protein are hallmarks of NMD, we treated cells expressing miniμ C3/C4 constructs with the translation inhibitor cycloheximide (CHX) before RNA analysis or depleted the cells of Upf1. Both miniμ C3/C4 ter440 and miniμ C3/C4 ter452 mRNA levels were restored to miniμ C3/C4 WT mRNA levels upon CHX treatment (**Supplementary Fig. 2** online) and upon depletion of Upf1 using RNA-mediated interference (RNAi) techniques (**Fig. 1c**), demonstrating that these transcripts are recognized and degraded by NMD.

To assess the role of EJCs in NMD of miniμ and miniμ C3/C4 constructs, we knocked down eIF4AIII, which is an mRNA-binding core EJC factor<sup>10</sup>. Under conditions that resulted in a five-fold or greater reduction of the eIF4AIII protein (**Fig. 1d**, gel), NMD of miniμ ter452, miniμ C3/C4 ter440 and miniμ C3/C4 ter452 was

not affected, consistent with the expectation that these mRNAs should not contain an EJC bound downstream of the PTC. In contrast, miniμ ter440 lost its efficient mRNA downregulation upon eIF4AIII knockdown, but still produced two- to three-fold lower mRNA levels than the miniμ WT construct. This remaining mRNA downregulation is consistent with the hypothesis that NMD in mammals is generally EJC-independent, as in *Saccharomyces cerevisiae*<sup>11</sup>, *Caenorhabditis elegans* (J. Caceres, MRC Edinburgh, personal communication) and *Drosophila melanogaster*<sup>12</sup>, but that the presence of an EJC downstream of the PTC functions as an enhancer of NMD.

For NMD of β-globin mRNA, it has been reported that the last exon has a so-called 'fail-safe sequence' that allows for PTC recognition in the absence of a downstream intron<sup>5</sup>. To determine whether Ig-μ contains such a fail-safe sequence, we deleted the sequence of exon C4 until immediately upstream of the normal termination codon (miniμ C3, **Fig. 2a**). As a control, we substituted the exon C4 sequence with a sequence of identical length from the histone H4 coding region (miniμ C3/H4). We chose the histone H4 sequence because it has been shown that this mRNA is immune to NMD and therefore should not contain any putative fail-safe sequences<sup>13</sup>. Whereas no NMD was observed with miniμ C3 (**Fig. 2a**), the mRNA level of miniμ C3/H4 ter440 was reduced similarly to miniμ C3/C4 ter440 (**Fig. 2a**), and this reduction was dependent on Upf1 (**Fig. 2b**). These results indicate that the distance between the termination codon and some unknown feature in the 3' untranslated region (UTR) is a crucial determinant for NMD and that the coding region of exon C4 does not contain any special *cis*-acting signal required for the observed EJC-independent NMD. In yeast, recent data shows that the distance between the termination codon and the poly(A) tail can determine whether an mRNA is shunted to the NMD pathway or not<sup>11,14</sup>. If the same mechanism exists in mammals, it should be possible to convert our PTC-free miniμ WT mRNA into an NMD substrate by extending the 3' UTR. Indeed, a construct termed miniμ long 3' UTR, which has inserted into the 3' UTR a 1.3-kilobase stuffer sequence, gave a five-fold lower mRNA level compared to the parental miniμ construct (**Fig. 2c**). Knockdown of human Upf1 using RNAi techniques resulted in an increase of miniμ long 3' UTR mRNA by four-fold, reaching 70% of the mRNA level of the parental miniμ (**Fig. 2c**). Thus, increasing the distance between the

termination codon and the poly(A) tail in *miniμ* leads to a Upf1-dependent mRNA downregulation.

In summary, the results presented here are incompatible with the current model for mammalian NMD, according to which recognition of a PTC strictly relies on an interaction between the terminating ribosome and an EJC located downstream of it<sup>2</sup>. Instead, we find that the distance between the termination codon and the poly(A) tail seems to be an important determinant for EJC-independent NMD in Ig- $\mu$ . Long 3' UTRs are also known to trigger NMD in yeast and *C. elegans*<sup>14,15</sup>. Our results are consistent with yeast NMD models, which posit that proper translation termination can only occur in the appropriate local mRNP context<sup>11,16</sup>. If a yeast ribosome encounters a termination codon or stalls for other reasons in the 'wrong' local mRNP environment, the mRNA will be degraded in a Upf1p-dependent manner. In yeast, such aberrant NMD-inducing translation termination can be rescued by tethering poly(A)-binding protein (PABP) downstream of the PTC<sup>11</sup>, suggesting that PABP interaction with terminating ribosomes might be a conserved requirement for correct translation termination. Although a role for PABP in mammalian NMD remains to be demonstrated, our results suggest an NMD model where PTC recognition is EJC independent, evolutionary conserved and accomplished as described above, and where the presence of an EJC downstream of the termination codon functions as an enhancer of NMD in mammals.

Note: Supplementary information is available on the Nature Structural & Molecular Biology website.

#### ACKNOWLEDGMENTS

We thank J. Lykke-Andersen, J. Lingner, M.J. Moore, A. Kulozik and L.E. Maquat for antibodies and plasmids. This work was supported by the Kanton Bern and by grants to O.M. from the Swiss National Foundation, the Novartis Foundation for Biomedical Research and the Helmut Horten Foundation.

#### COMPETING INTERESTS STATEMENT

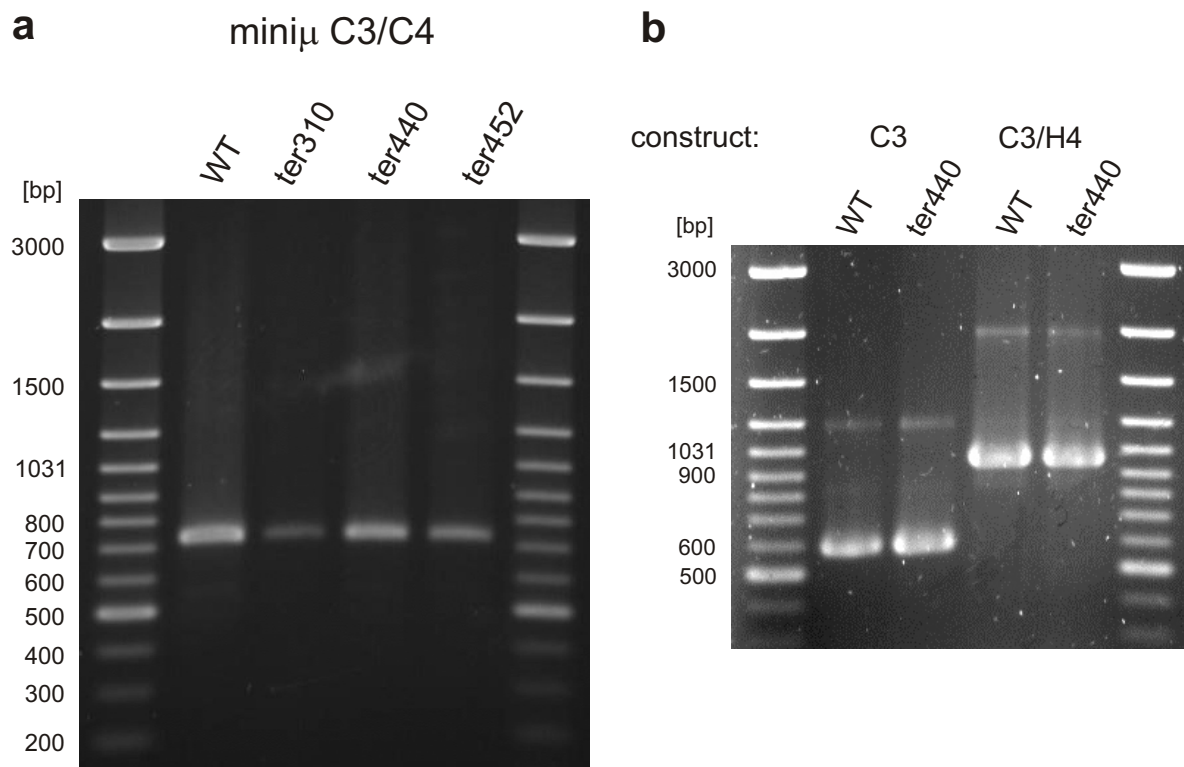
The authors declare that they have no competing financial interests.

Published online at <http://www.nature.com/nsmb/>

Reprints and permissions information is available online at <http://npg.nature.com/reprintsandpermissions/>

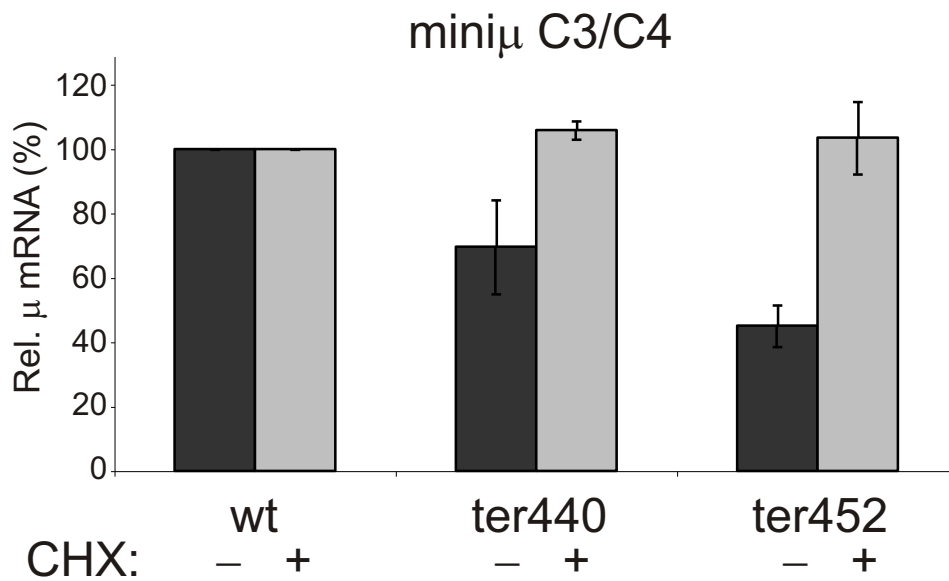
1. Conti, E. & Izaurralde, E. *Curr. Opin. Cell Biol.* **17**, 316–325 (2005).
2. Maquat, L.E. *Nat. Rev. Mol. Cell Biol.* **5**, 89–99 (2004).
3. Buhler, M., Paillusson, A. & Muhlemann, O. *Nucleic Acids Res.* **32**, 3304–3315 (2004).
4. Carter, M.S., Li, S. & Wilkinson, M.F. *EMBO J.* **15**, 5965–5975 (1996).
5. Zhang, J., Sun, X., Qian, Y. & Maquat, L.E. *RNA* **4**, 801–815 (1998).
6. Rajavel, K.S. & Neufeld, E.F. *Mol. Cell. Biol.* **21**, 5512–5519 (2001).
7. Delpy, L., Sirac, C., Magnoux, E., Duchez, S. & Cogne, M. *Proc. Natl. Acad. Sci. USA* **101**, 7375–7380 (2004).
8. Chan, D., Weng, Y.M., Graham, H.K., Sillence, D.O. & Bateman, J.F. *J. Clin. Invest.* **101**, 1490–1499 (1998).
9. LeBlanc, J.J. & Beemon, K.L. *J. Virol.* **78**, 5139–5146 (2004).
10. Shibuya, T., Tange, T.O., Sonenberg, N. & Moore, M.J. *Nat. Struct. Mol. Biol.* **11**, 346–351 (2004).
11. Amrani, N. *et al. Nature* **432**, 112–118 (2004).
12. Gaffield, D., Unterholzner, L., Ciccarelli, F.D., Bork, P. & Izaurralde, E. *EMBO J.* **22**, 3960–3970 (2003).
13. Maquat, L.E. & Li, X.J. *RNA* **7**, 445–456 (2001).
14. Muhrad, D. & Parker, R. *RNA* **5**, 1299–1307 (1999).
15. Pulak, R. & Anderson, P. *Genes Dev.* **7**, 1885–1897 (1993).
16. Hilleren, P. & Parker, R. *RNA* **5**, 711–719 (1999).

## Supplementary Figure 1



**Supplementary Figure 1** The various miniμ constructs are spliced as predicted (**a**) RT-PCR analysis of the miniμ C3/C4 mRNAs measured in **Figure 1b** to check for induction of aberrant splicing between exon C2 and C4. PCR products were resolved on a 1.5% agarose gel and stained with ethidium bromide. Correct splicing gives an amplicon of 722 base pairs. (**b**) RT-PCR analysis of the miniμ C3 and miniμ C3/H4 mRNAs measured in **Figure 2a** was performed to check for aberrant splicing between exon C2 and the 3' UTR as in a. Correct splicing gives amplicons of 590 and 972 base pairs for miniμ C3 and miniμ C3/H4, respectively.

## Supplementary Figure 2



**Supplementary Figure 2** Downregulation of PTC+ miniμ C3/C4 mRNA depends on translation. HeLa cells transfected with the indicated miniμ C3/C4 constructs and a β-globin expressing plasmid<sup>3</sup> for normalization were harvested 48 h post transfection (dark bars) or treated with 100 μg/ml cycloheximide (CHX; light bars) for 2 h before harvesting. Relative mRNA levels, normalized to relative β-globin mRNA, were determined by real-time RT-PCR as in **Fig. 1b**. Average mRNA levels and standard deviations from three real-time PCR runs are indicated.

## Supplementary Information

### Material and Methods

**Plasmids.** The Ig- $\mu$  minigenes mini $\mu$ wt, mini $\mu$ ter310, mini $\mu$ ter440 and mini $\mu$ ter452 are described elsewhere <sup>1</sup>. Fusion PCR was used to delete the intron between exons C3 and C4 (giving mini $\mu$  C3/C4), and to delete the coding region of exon C4 (giving mini $\mu$  C3). For mini $\mu$  C3/H4, a 378 base pairs long fragment of mouse histone H4 (spanning from 56 base pairs upstream of the ATG to the C-terminal amino acid) was amplified with primers introducing an Eco R1 site and inserted in-frame into the EcoR1 site of mini $\mu$  C3. This histone H4 fragment does not contain any in-frame TCs. The 1.3 kb stuffer fragment comprising 24 MS2 binding sites in mini $\mu$  long 3' UTR was excised from pSLx24 <sup>2</sup> using Bam H1 and Bgl II and inserted into the BamH1 site in the 3' UTR of mini $\mu$ wt <sup>1</sup>. The sequence of the entire ORF in each construct was confirmed by sequencing. Sequences of all oligonucleotides used for cloning and sequencing are available on request.

**Transfections and real-time RT-PCR.** HeLa cells were grown in 6-well plates and transiently transfected with 100 - 150 ng mini $\mu$  constructs-encoding plasmid DNA using 3  $\mu$ l LipofectAmine (Invitrogen) or 2  $\mu$ l DreamFect (OZ Biosciences). For normalization, 150 – 200 ng of a  $\beta$ -globin encoding plasmid <sup>3</sup> was co-transfected in **Figures 1c, 2a** and **Suppl. Fig. 2**, and 150 ng of a rat GPx1 encoding plasmid <sup>4</sup> was co-transfected in **Figures 1d, 2b** and **2c**. 48 h post-transfection (or later for RNAi experiments, see below), cells were harvested and RNA was isolated with “Absolutely RNA<sup>TM</sup> RT-PCR Miniprep

Kit” (Stratagene). Subsequently, 1 µg RNA was reverse transcribed in 50 µl Stratascript first strand buffer in the presence of 0.4 mM dNTPs, 300 ng random hexamers, 40 U RNasIn (Promega) and 50 U Stratascript (Stratagene). For real-time PCR, reverse transcribed material corresponding to 40 ng RNA was amplified in 25 µl Universal PCR Master Mix, No AmpErase<sup>®</sup> UNG (Applied Biosystems) and with the primers and TaqMan probes described below. Ig-µ mRNA was measured over the exon junction C2/C3 with 800 nM 5'-GTCTCACCTTCTTGAAGAACGTGTC-3', 800 nM 5'-GGGATGGTGAAGGTTAGGATGTC-3' and 200 nM 5'-FAM-CACATGTGCTGCCAGTCCCTCCAC-TAMRA-3'. Neomycin mRNA was measured with 800 nM 5'-TGTGACATAATTGGACAAACTACCTACA-3', 800 nM 5'-CAT TCCACCACTGCTCCCA-3' and 200 nM 5'-FAM-AGATTTAAAGCTCTAAGATT CCAACCTATGGAAGTGA -TAMRA-3'. β-globin mRNA was measured with 800 nM 5'-GCTGCACTGTGACAAGCTGC-3', 800 nM 5'-AAAGTGATGGGCCAGCACAC-3' and 200 nM 5'-FAM-TCCTGAGAACTTCAGGCTCCTGGGCAAC-TAMRA-3'. GPx1 mRNA was measured with 800nM 5'-TGGTGGTGCTCGGTTTCC-3', 800nM 5'-GACATACTTGAGGGAATTCAGAATCTC-3' and 200nM 5'-FAM-CCATTCTCCTGATGTCCGAACTGATTGC-TAMRA-3'. hUpf1 and eIF4AIII mRNAs were measured with assay-on-demand reagents Hs00161289\_m1 and Hs00207168\_m1, respectively, and GAPDH with pre-developed assay reagents (PDAR) from Applied Biosystems. Real-time PCR was run on the GeneAmp 7000 Sequence Detection System (Applied Biosystems) using the standard thermal profile. Relative Ig-µ mRNA levels were normalized either to neomycin mRNA (**Fig. 1b**), to β-globin mRNA (**Figs. 1c, 2a**

and **Suppl. Fig. 2**), or to GPx1 mRNA (**Figs. 1d, 2b and 2c**), and are shown relative to the PTC-free version (wt) of each construct, which were set to 100%. Average values and standard deviations of 3 - 8 real-time PCR runs with cDNAs of one representative experiment are shown.

**RNAi.** Knockdown of hUpf1 by RNAi was induced by co-transfection with the reporter plasmids of totally 300 - 400 ng of an equimolar mix of pSUPERpuro plasmids targeting two different sequences in hUpf1 <sup>5</sup>. 24 h after transfection, untransfected cells were eliminated by culturing the cells in the presence of 1.5 µg/ml puromycin for 48 h. Cells were then washed in PBS and incubated in puromycin-free medium for another 24 h. Total RNA was isolated and whole cell lysates for western blotting were prepared after totally 96 h post transfection. For knocking down eIF4AIII, 1x10<sup>6</sup> cells were seeded in 10 cm dishes. The next day, 5 µg pSUPERpuro-eIF4AIII targeting the sequence 5'-CGAGCAATCAAGCAGATCA-3' was cotransfected with 150 ng miniµ-encoding plasmid DNA and 150 ng pmCMV-rGPx1-TGC <sup>4</sup>. 24 h after transfection, 3 µg/ml puromycin was added for 30 h to eliminate untransfected cells. Before harvesting 72 h post transfection, cells were incubated in puromycin-free medium for 18 h. As a mock control, empty pSUPERpuro vector <sup>5</sup> was used in **Fig. 1c**, and pSUPERpuro-scrambled (unspecific "target" sequence 5'-ATTCTCCGAACGTGTCACG-3') was used in **Figs. 1d and 2**. In all RNAi experiments, the efficiency of the knockdown was assessed on the mRNA level by real-time RT-PCR (not shown) and on the protein level by western blotting.

**Western blotting.** Whole cell lysates corresponding to  $5 \times 10^4 - 2 \times 10^5$  cells per lane were electrophoresed on a 10% SDS-PAGE. Protein was transferred to Optitran BA-S 85 reinforced nitrocellulose (Schleicher & Schuell) and probed with 1:2500 diluted polyclonal rabbit anti-hUpf1 antiserum <sup>6</sup>, 1:1000 diluted affinity-purified polyclonal rabbit anti-eIF4AIII antibody <sup>7</sup> or 1:1000 diluted monoclonal mouse anti-lamin A/C antibody (Santa Cruz Biotechnology). 1:2500 diluted HRP-conjugated anti-rabbit or anti-mouse IgG (Promega) was used as secondary antibody. ECL+ Plus western blotting detection system (Amersham) was used for detection and signals were visualized on a Luminescent Image Analyzer LAS-1000 (Fujifilm).

**Endpoint RT-PCR.** Total cellular RNA was isolated and reverse transcribed as described above, except that 6 ng/ $\mu$ l of oligo 5'-(dT)<sub>30</sub>VN-3' was used instead of random hexamers. Reverse transcribed material corresponding to 60 ng total RNA was amplified with "PCR Core Kit" (Qiagen), forward primer 5'-GCTGAACCTGAATGTGTAACCTGCCGTGTGGATCAC-3' and reverse primer 5'-AGCGCCTAGGCTCTCGGTCACCAGGTGTGGCAG-3' to analyze the C2/C3/C4 region of mini $\mu$  C3/C4 (**Suppl. Fig. 1a**). For analysis of the C2/C3 region in mini $\mu$  C3 and the C2/C3/H4 region in mini $\mu$  C3/H4, cDNA corresponding to 200 ng total RNA was amplified as above using the forward primer indicated above and reverse primer 5'-CATCGAATGCATGGATCCAGCAGGCATGAGCATTGTATAATC-3' (**Suppl. Fig. 1b**). RT-PCR products were separated on a 1.5% agarose gel and cloned into the TOPO vector pCRII (Invitrogen) for subsequent sequencing

## Supplementary References

1. Buhler, M., Paillusson, A. & Muhlemann, O. *Nucleic Acids Res* **32**, 3304-15 (2004).
2. Fusco, D. et al. *Curr Biol* **13**, 161-7. (2003).
3. Thermann, R. et al. *EMBO J* **17**, 3484-94 (1998).
4. Moriarty, P.M., Reddy, C.C. & Maquat, L.E. *RNA* **3**, 1369-1373 (1997).
5. Paillusson, A., Hirschi, N., Vallan, C., Azzalin, C.M. & Muhlemann, O. *Nucleic Acids Res* **33**, e54- (2005).
6. Lykke-Andersen, J., Shu, M.D. & Steitz, J.A. *Cell* **103**, 1121-31. (2000).
7. Shibuya, T., Tange, T.O., Sonenberg, N. & Moore, M.J. *Nat Struct Mol Biol* **11**, 346-51 (2004).